J Mater Sci (2007) 42:7488–7493
DOI 10.1007/s10853-006-1463-z

Mixing in Au/Ge system induced by Ar^+ ion irradiation

**J. M. Nawash · N. M. Masoud · K. A. Al-Saleh ·
N. S. Saleh**

Received: 7 May 2006 / Accepted: 15 December 2006 / Published online: 18 May 2007

Abstract Rutherford Backscattering Spectrometry (RBS) and Electrical Resistivity Measurements (ERM) were used to investigate the mixing of Au/Ge bilayer deposited onto glass substrate induced by Ar ions. Mixing was initiated by bombarding the sample with 400 keV $^{40}Ar^+$ beam with a fluence up to 1.2×10^{17} ions/cm^2 at a constant flux of 0.25 μA/cm^2. To assist the evaluation of the experimental results, all spectra were simulated using ''RUMP'' computer code. RBS results indicated that ion beam mixing led to a formation of $AuGe_2$ compound. The mixed region was noticed to increase with the gradual increase of Ar^+ fluence. Results were also compared with current theoretical models used to describe the mixing process. The Bϕrgesen thermal spike model was found to accurately predict the diffusion in Au/Ge interface. An increase in the electrical resistivity of the film was detected during Ar^+ irradiation.

Introduction

Using a selected ion beam with energies ranging from tens to hundreds of keV, ion implantation technique allows the introduction of any element into any solid independent of thermodynamic constraints. The process has proved to be a highly versatile and controllable method for modifying the composition, structure, and properties (optical, mechanical, and electrical) of the near surface region of many materials [1, 2]. However, direct implantation has some disadvantages limiting its applications, e.g. the limitation imposed by the sputtering effect in relation to the maximum obtainable composition, makes it impossible to induce changes in various novel systems, especially if the source material is not available. Alternatively, the novel technique of ion beam mixing (IM) has successfully been applied to a wide variety of scientific fields and industrial applications to obtain non-equilibrium alloys [3–6]. In contrast to direct implantation, the inert gas ion beam is used to trigger atomic collisions to induce intermixing between deposited material B and the matrix A, or both deposited A and B bilayer or multilayer on a substrate, to form a uniform A–B alloy phase [7].

Ion beam mixing is of interest in the study of beam-assisted growth for both metals and semiconductors. It has been shown to be a simple method for producing thin metal films of new structures that are not easily formed by other techniques. Also, it has a great potential for improving wear or corrosion resistance of metals. In semiconductors, it is a promising technique used to combine a metal layer with a semiconductor for preparation of electrical contacts, and it has been demonstrated to be a useful procedure for dispersal of impurities prior to film growth. In addition to these fields, studies of IM yield important information about the fundamental mechanisms of the interactions of ions with solids [8].

Although numerous experiments have been conducted on ion beam mixing, extensive work still needs to be done to understand the mechanisms involved in mixing on an

---

J. M. Nawash · N. M. Masoud (✉) · K. A. Al-Saleh ·
N. S. Saleh
Physics Department, University of Jordan, Amman, Jordan
e-mail: masoudn@wpunj.edu

Present Address:
J. M. Nawash
Material Research Center, Washington State University,
Pullman, WA, USA

Present Address:
N. M. Masoud
UV Solutions Inc., Newark, NJ, USA

atomic level. Several models have been proposed to study the fundamental processes. However, the mixing rate under heavy ion bombardment cannot be explained in some systems. In these cases, the cascade mixing mechanism alone cannot sufficiently predict the mixing, and thermal spike and/or radiation enhanced diffusion are believed to play an important role in the process.

Ballistic mixing is defined as all processes initiated by direct collision [9, 10]. It is divided into two main categories: projectile-target collision (knock-on) and recoil-target collision (cascade) [11]. When the individual ion cascades are sufficiently dense and long-lived, the energy deposited is large enough so that it is thermalized, and the volume of a solid in which the temperature is localized is known as thermal spike [12]. Consequent to ion irradiation, a large concentration of mobile points and cluster defects are formed leading to a net atomic transport within the material. This migration is a result of a temperature gradient caused when the initial cascade has reached thermal equilibrium, thus radiation enhanced diffusion (RED) is simply an enhancement of normal thermal diffusion by virtue of the ion irradiation process [13].

Ion beam induced mixing in Au/Ge bilayer has been reported many times in the literatures [14–17]. Bhattacharya et al. [14, 15] attempted the synthesis of Au–Ge alloy by low energy Si ion beam mixing without success. RBS measurements done by Som et al. [16, 17] have shown no significant intermixing in Au/Ge bilayer system due to 120 MeV Au ions irradiation at room temperature. However, high-resolution transmission electron microscopy (TEM) studies have shown the formation of nanocrystalline seeds of $Au_{0.6}Ge_{0.4}$ alloy [17]. When the irradiated Au/Ge sample was vacuum annealed at a temperature of 360 °C for 5 h, a formation of *a*-axis oriented islands of $Au_{0.6}Ge_{0.4}$ alloy was observed. In this work, the Au/Ge system is studied at room temperature to enrich the data available on bilayer systems, and to a certain extent, to examine the theoretical models mentioned above. On the other hand, the resistivity of the formed region was measured and the effect of mixing on electrical properties of the Au/Ge system was studied.

Experimental

The Au/Ge bilayer film was vacuum deposited onto a glass substrate. A Leybold evaporator was used for sample preparation. It was equipped with a calibrated quartz oscillator for thickness and evaporation rate monitoring. Pure gold and germanium were evaporated from tungsten crucibles with a mean evaporation rate of 5 Å/s. Samples, for resistivity measurements, were prepared using a masking technique. A germanium layer 1,400 Å thick with lateral dimensions 1.4×0.3 cm^2 was deposited on a glass substrate. For the resistivity measurements, silver contacts were deposited on both sides of the substrate so that they touch the germanium film on both sides. Then a gold layer 400 Å thick with the same lateral dimensions as the germanium film was deposited on the top. The Au-film thickness was chosen to be about one-third of the projected range (evaluated based on TRIM-97 calculations [18]) of 400 keV Ar$^+$ ions in this film to insure that most of the incident ions cross the Au/Ge interface and stop in the Ge layer.

For ion beam irradiation, the target was mounted in a vacuum chamber pumped to 10^{-5} mbar. Ion mixing was then initiated by 400 keV Ar$^+$ ions at room temperature with a beam flux of 1.4×10^{12} (ion/cm^2 s). The fluence was progressively varied until a maximum fluence of 1.2×10^{17} ions/cm^2 was reached. The fluence was measured by a current beam integrator.

For analysis, Rutherford Backscattering Spectrometry (RBS) technique was carried out using a 2 MeV He^{+4} beam. The backscattered particles were collected using a Si-surface barrier detector with a resolution of 17 keV. The detector was mounted to collect ions scattered at an angle of 135°. Both Ar$^+$ and He^{+4} beams were supplied from Jordan Van de Graaff Accelerator (JOVAC) at the University of Jordan. In situ resistance measurements were carried out using the component evaluation technique by means of ac-voltage and current measurements utilizing a lock-in-amplifier. Resistance and RBS measurements were carried out after each irradiation. Conventional electronics were used to condition and amplify the signal. RBS data was then analyzed using a computer code ‘‘RUMP’’ [19] and an IBM microcomputer. Details of the analysis are given in references [20, 21]. More detailed information about the backscattering system is available elsewhere [22–24].

Results and discussion

Figure 1 shows a typical RBS energy spectrum using 2 MeV He^{+4} on the as-deposited Au/Ge bilayer system. The solid curve represents the corresponding simulation generated using RUMP computer code. Clearly, the as-deposited spectrum reveals a normal surface scattering with an energy position as expected from RBS kinematics. The shift in the Ge edge towards lower energies by some 56 keV is due to energy loss through the Au film and corresponds to the nominal deposited film thickness of 400 Å. No foreign impurities were detected. This means that the deposition was carried out under typical working conditions in a free and clean environment. Figure 1 illustrates an excellent match between the measured and calculated spectra.

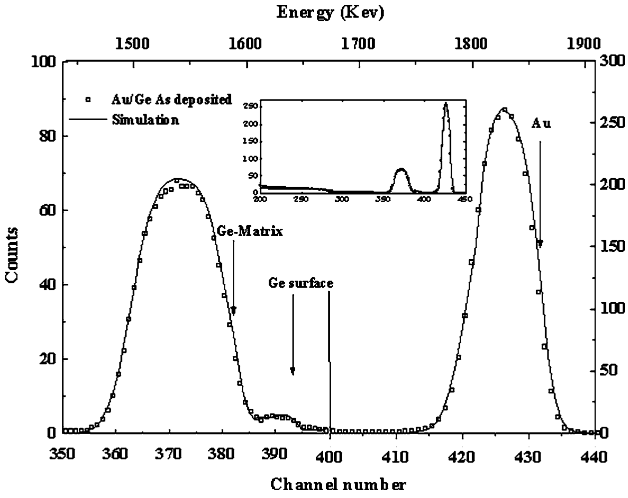

Fig. 1 Typical 2 MeV $^4He^+$ spectrum as a result of scattering from Au/Ge system. The solid curve represents the simulation as obtained from RUMP calculations. For clarity, we have used two different scales for Au (left) and Ge (right). The inset shows the entire spectrum including the glass substrate, the Ge and the Au peaks all at the same scale

Figure 2 shows the RBS spectra of Au/Ge samples irradiated at room temperature with Ar^+ fluences of 7.6×10^{16} ions/cm^2 (circles) and 1.2×10^{17} ions/cm^2 (triangles). The as-deposited spectrum (squares) is shown for comparison. The RBS energy spectra illustrate that the interface region is functionally dependent on the imparted Ar^+ fluence. The Ar ion irradiation is seen to cause simultaneous mixing across the Au/Ge interface, where a broadening of the Au peak toward lower energies occurred, and the front edge of the Ge peak extended toward higher energies with increasing Ar ion fluence. This indicates that the Au atoms diffused through the Ge layer as the Ge atoms diffused into the Au film. On the other hand, the reduction in the height of both Au and Ge signals corresponds to the movement of both Au and Ge atoms. It is noticed that the amount of Au atoms, which is proportional to the area under the Au peak, is not reduced with Ar^+ fluence. This means that sputtering of Au atoms is negligible under these relatively low fluences.

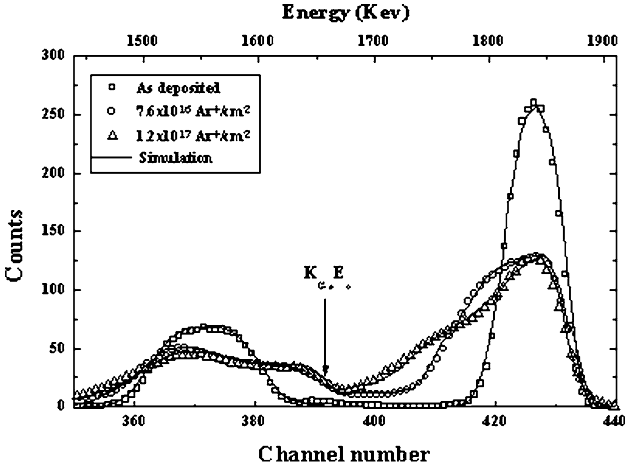

Fig. 2 RBS spectra illustrating the variations observed against the accumulative fluence up to 1.2×10^{17} Ar^+/cm^2. The as-deposited spectrum is shown for comparison. The solid curves represent the calculated spectra obtained from computer code RUPM

Results show that the mixing at the Ag/Ge interface occurred as a function of Ar^+ fluence. At a fluence of 1×10^{17} ions/cm^2 and higher the front edge of the Ge step is shifted to an energy of $K_{Ge}E_0$, where K_{Ge} is the kinematic factor, which is defined as the ratio between the projectile energy after the elastic collision (E_1) and the energy before the collision (E_0). The shift of the Ge step to $K_{Ge}E_0$ indicates that Ge atoms have moved up to the surface of the Au film. This is an indication that complete mixing took place and saturation was reached. On the other hand, the shape of both the front edge of the Ge step and the back edge of the Au peak have changed to a defined step like structure indicating a compound formation in the interface.

All experimental data were simulated using a standard computer code ''RUMP''. In all cases in the present study, as expected from interdiffusion processes, the backscattering yield is parameterized by the error function like concentration profiles of the form [25]:

$$C(x) = C_0\left\{1 - \operatorname{erf}\left[(x - d)\Big/\sqrt{2\sigma}\right]\right\}\Big/2$$

where $\sigma 2(\Phi)$ is the variance and $d(\Phi)$ is the actual location of the interface. Examples of the simulation (solid curves), conducted after Ar^+ irradiation, are illustrated in Fig. 2. The figure indicates excellent agreement between the measured and the calculated spectra. The results of simulations made by the RUPM code enabled us to calculate the stochieometry of the resulting compound of the mixed layer formed which is found to be $AuGe_2$ with a thickness of 730 Å. It must be pointed out that other studies of ion beam mixing in Au/Ge system indicated a formation of a range of compounds under different bombardment conditions [16, 17]. Other compounds have also been formed in metal/Ge and metal/Si bilayers. For example, Dhar et al. [26] have shown a formation of Cu_3Ge and Co_2Ge phases during ion beam mixing of Cu/Ge and Co/Ge systems at room temperature using 1 MeV Kr^+ ions. Lau et al. [27] reported that a layer of Au_5Si_2 was obtained by irradiating a thin layer of Au on Si, at room temperature, with 300 keV Xe ions.

It is well known that atomic transport processes initiated by IM are usually divided into an athermal regime and a temperature-dependent regime. The atomic transport in the latter regime is caused by the radiation enhanced diffusion (RED) process, while the atomic transport in the athermal regime is due to collisional cascade and/or thermal spike processes. This implies that the cascade model alone cannot properly describe the IM at low temperatures [3]. According to Auner et al. [28], the relative importance of the ballistic and the thermal spike contributions is influenced by the amount of cohesive energy. Atomic transport in the bilayer, which has a higher average cohesive energy (>7 eV) can be explained by a ballistic contribution, while atomic transport in the bilayer with a lower average cohesive energy (<6 eV) can be explained by thermal spike effects. As the average cohesive energy in the Au/Ge bilayer is about 3.8 eV, we conclude that the atomic transport in this system might be due to a thermal spike process.

On the other hand, criteria for the applicability of thermal spike models were derived by Cheng [29] and Bolse [30] in terms of the average atomic number, Z_{ave}, and the deposited recoil energy, F_D. Collision cascades in a target material with atomic number $Z_{\text{ave}} > 20$ may become space filling as soon as the kinetic energy transferred to the recoil atoms is less than the spike-initiation threshold. As this will occur at the end of the sub-cascades, spatially separated local thermal-spike effects will occur away from the direct ion trajectory. In this hot and probably molten zone, fast transient atomic transport processes may take place. Such transient diffusion processes may be chemically driven and strongly enhanced as compared to ballistic mixing. However, it is found that low temperature IM of materials with $Z_{\text{ave}} < 20$ is a purely ballistic process without influence of any chemical driving forces. For higher atomic numbers, mixing occurs by chemically biased diffusion in spatially separated local thermal spikes. On the other hand, it was found that for a deposit recoil energy F_D above a critical value of about 2.1 keV/nm, global spikes are expected to be formed, whereas below this value the formation of a local thermal spike is more likely. Based on this argument, the conditions in our system with $Z_{\text{ave}} = 55.5$ and $F_D = 0.69$ keV/nm (which is much lower than the critical value) strongly favor the formation of local thermal spikes.

To quantify the mixing in the Au/Ge system, the values of the mixing rate parameter, namely $\frac{4Dt}{\Phi}$, for both Au and Ge are first determined experimentally and then evaluated theoretically based on the available theoretical models. Consequently, one may compare the determined value with theory and attribute the mixing mechanism to either collisional cascade, thermal spike (Johnson or Bϕrgesen), or RED models. A collective mechanism arising from more than one model may also be possible. This, however, depends on the system studied, the energy and type of beam species that initiate mixing, and its fluence and fluence rate. The mixing parameter was experimentally determined from each spectrum at the respective Ar$^+$ fluences by [31]:

$$4Dt = 2\left\{\sigma^2(\phi) - \sigma^2(0)\right\}$$

where $\sigma^2(0)$ and $\sigma^2(\phi)$ are, respectively, the measured variances before and after irradiation. The variances are determined by calculating half the energy (or equivalent depth) corresponding to a drop of peak intensity from 84% to 16% after correcting for the Bohr energy straggling and system resolution.

Figure 3 shows a plot of the mixing parameter, 4Dt against the Ar$^+$ fluence, ϕ, for both Au and Ge. The experimental data exhibit a linear dependence on the Ar$^+$ fluence. From the plots, one can extract the corresponding rates of mixing, i.e., $d(4Dt)/d\Phi$, by fitting straight lines through the experimental points. The data reveal mixing rates (the slope of each straight line) of $(1.9 \pm 0.4) \times 10^4$ Å^4, and $(6.1 \pm 0.9) \times 10^4$ Å^4 for Au and Ge, respectively. We have also calculated the mixing efficiency, defined as the ratio of the mixing parameter to the energy, F_D, deposited at the interface per unit length, namely $\left(\frac{4Dt}{\Phi F_D}\right)$, which is independent of the bombardment conditions. Based on the TRIM calculations we have determined the average value of F_D at the Au/Ge interface as 69.4 eV/Å. The corresponding mixing efficiencies for Au and Ge are, respectively equal to 275.2 Å^5/eV and 873.2 Å^5/eV.

Table 1 shows the theoretical values of the mixing rate parameter for Au/Ge system. The binary collision cascade model proposed by Sigmund and Gras-Marti [10], gave a mixing rate of 8.40×10^2 Å^4 (4.06×10^3 Å^4) and a mixing efficiency of 12.1 Å^5/eV (58.5 Å^5/eV) for Au (Ge). These values are smaller in magnitude than experimental values, which implies that the cascade process is not the dominant mixing mechanism for both Au and Ge.

The global thermal spike model of Johnson et al. [32] predicts a mixing rate and efficiency of 2.47×10^3 Å^4 and 35.6 Å^5/eV. The corresponding values obtained, based on the Bϕrgesen model [33, 34], which assumes local

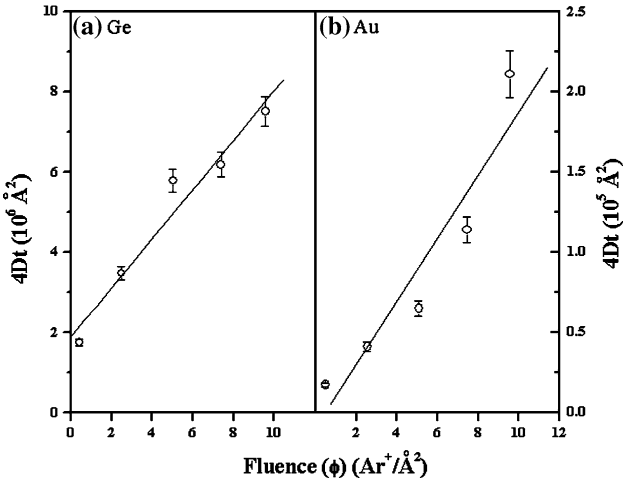

Fig. 3 Dependence of the interdiffusion parameter, 4*Dt*, on the imparted Ar$^+$ fluence. Data are for germanium in (**a**) and gold in (**b**)

Table 1 Values of the mixing rate parameter, $(4Dt)/\phi$, for both Au and Ge based on theoretical predictions in the Au/Ge system

<table>
<tr><th rowspan="2">Model</th><th colspan="2">Mixing rate parameter $(4Dt)/\phi$ ($Å^4$)</th></tr>
<tr><th>Au atoms</th><th>Ge atoms</th></tr>
<tr><td>Cascade</td><td>8.40×10^2</td><td>4.06×10^3</td></tr>
<tr><td>Thermal Spike (Johnson)</td><td colspan="2">2.47×10^3</td></tr>
<tr><td>Thermal Spike (Bϕrgesen)</td><td colspan="2">2.12×10^4</td></tr>
<tr><td>RED (Myer)</td><td>8.70×10^{10}</td><td>4.70×10^{16}</td></tr>
<tr><td>Experiment</td><td>1.91×10^4</td><td>6.06×10^4</td></tr>
</table>

spherical spike formation at the ends of individual recoil cascades, are respectively 2.12×10^4 $Å^4$ and 305.5 $Å^5$/eV. This result is in good agreement with the experimental value for Au, but it is about a factor of 3 smaller than that calculated for Ge. Lastly, the values of mixing rate parameter and efficiency as predicted from Myers model [13] which is based on radiation enhanced diffusion (RED), are, respectively, 8.70×10^{10} $Å^4$ and 1.3×10^9 $Å^5$/eV (4.70×10^{16} $Å^4$ and 6.8×10^{14} $Å^5$/eV) for Au (Ge). These values are much higher than the experimental values. It should be mentioned that cascade and thermal spike models are considered to be independent of temperature, i.e., they describe the athermal ion mixing regime, while RED is the mechanism described in the thermal ion-beam mixing regime, that has a temperature dependent behavior [35].

Our experimental values of the mixing rate for both Au and Ge are comparable to the values obtained by the Bϕ regesen thermal spike model, i.e., Au and Ge atoms diffuse across the Au/Ge interface via the Bϕregesen thermal spike. Figure 2 also reveals that the tails of both Au and Ge peaks are short, this implies that only short range transport mechanisms are involved in thermal spike mixing for both Au and Ge layers.

Many optical, mechanical and electrical properties of the mixed region can be modified as a result of mixing. Resistivity is used as an example to check the effect of mixing on the electrical properties of the mixed region. The resistivity of the sample is sensitive to defects produced by ion irradiation, so one expects that it varies during the experiment. An ac-component method is used to measure the changes of the sample resistivity, $\Delta\rho$, as a function of the Ar^+ fluence, ϕ.

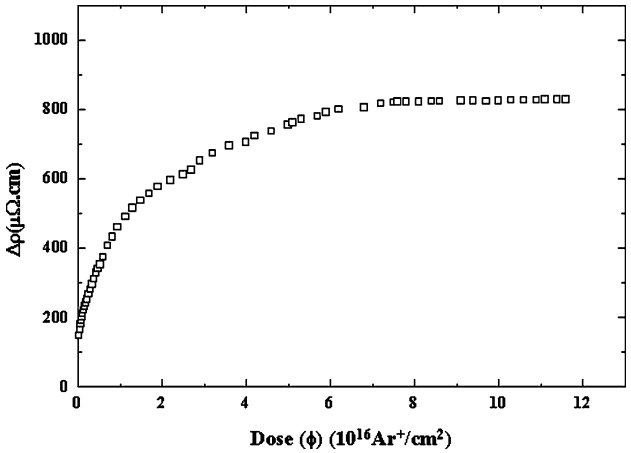

Fig. 4 The change in the electrical resistivity of the Au/Ge system versus fluence when bombarded with 400 keV Ar^+ ions

Figure 4 represents a plot of the change in resistivity, $\Delta\rho$, of the Au/Ge bilayer versus the Ar^+ fluence, ϕ. Three regimes can be recognized: First, up to a fluence of about 1×10^{16} ions/cm^2, a rapid increase in resestivity is mainly due to the production of point defects and defects clusters in the dense collision cascades and their subsequent overlapping [35]. The second regime is between 1×10^{16} and 1×10^{17} ions/cm^2, it corresponds to the mixing regime itself. Finally, a tendency toward a saturation process is reached above a fluence of 1×10^{17} ions/cm^2. This regime indicates the termination of the mixing process, in agreement with the RBS results.

Conclusions

The results obtained from the RBS and ERM measurements are in a good agreement. Both probes show that mixing takes place as the Ar^+ fluence increases, and a saturation of mixing occurs at a fluence of about 1×10^{17} ions/cm^2. The results of RBS show a formation of $AuGe_2$ stochieometric compound. Comparison between the experimental results and the available theoretical models reveals that both Au and Ge atoms diffuse through the interface via the Bϕrgesen thermal spike model. The mixing efficiency of the Ge atoms is found to be three times higher that that of Au atoms.

Acknowledgement We are grateful to Messrs. A. Khader, S. Kharabshah, A. Amre and S. Abdul-Rahman at the JOVAC facilities. We also would like to thank Frank D'Agosta for his help during the revision of the manuscript.

References

1. Riviere JP (1992) Nucl Inst and Meth B68:361
2. Joseph B, Mohapatra S, Satpati B, Lenka HP, Kuiri PK, Mahapatra DP (2005) Nucl Inst and Meth B227:559
3. Masoud NM, Arafah D-E, Becker KH (2002) Nucl. Inst. and Meth B198:64
4. Masoud NM, Arafah D-E (1999) Phys Stat Sol (a) 172:155
5. Arafah D-E, Masoud N, Mahmoud A (2002) Characterization of defects induced by $^{40}Ar^+$ beam irradiation in thin films used for solar cell devices, International Symposium on utilization of accelerators, Sao Paulo, Brazil, (November 2001), International Atomic Energy Agency (IAEA) Publications

6. Satpati B, Satyam PV, Som T, Dev BN (2004) Appl Phys A79:447
7. Liu BX, Jin O (1997) Phys. Stat. Sol. (a) 161:3
8. Paine BM, Liu BX (1989) In: Itoh T (ed) Ion beam assisted film growth. Elsevier, Amsterdam
9. Rossi F, Nastasi M (1991) J App Phys 69(3):1310
10. Sigmund P, Grass-Marti A (1985) Nucl Inst and Meth 182/183:25
11. Littmark U, Hofer WO (1980) Nucl Inst and Meth 168:329
12. Ibe E (1989) Nucl Inst and Meth B39:148
13. Myers SM (1980) Nucl Inst and Meth 168:265
14. Bhattacharya RS, Rai AK, Rashid H, Ezis A, Pronko PP (1985) In: Current MI, Sadana DK (eds) Proceedings of the International Society for Optical Engineering, vol 530, SPIE, Washington
15. Bhattacharya RS, Rai AK, Ezis A, Rashid MH, Pronko PP (1985) J Vac Sci Technol. A3:2316
16. Som T, Ayyub P, Kabiraj D, Kulkarni N, Kulkarni VN, Avasthi DK (2003) J Appl Phys 93:903
17. Som T, Satpati B, Satyam PV, Ayyub P, Kabiraj D (2003) Nucl Inst Meth B212:151
18. Ziegler JF, Biersack JP, Littmark N (1985) The stopping and ranges of ions in solids. Pergamon Press, New York
19. Doolittle LR (1985) Nucl Inst Meth B9:344
20. Chu WK, Mayer JW, Nicolet M-A (1978) Backscattering spectrometry. Academic Press, London
21. Knapp JA, Barbour JC, Doyyle BL (1992) J Vac Sci Technol A10(4):2685
22. Nawash J (1997) Ion beam mixing of some germanide systems, M.Sc. Thesis, Uneversity of Jordan, Amman, Jordan
23. Masoud N (1997) Ion beam mixing of Ag/Si system, M.Sc. Thesis, University of Jordan, Amman, Jordan
24. Al-Saleh KA, Saleh NS (1997) Phys Stat Sol (a) 161:407
25. Weber T, Lieb K-P (1993) J Appl Phys 37(7):3499
26. Dhar S, Kulkarni VN (1998) Thin Solid Films 333:20
27. Lau SS, Tsaur BY, von Allmen M, Mayer JW (1981) Nucl Instr Meth 182/183:97
28. Auner GW, Cheng YT, Alkais MH, Padnamabahn KR (1991) Appl Phys Lett 58:586
29. Cheng Y-T (1990) Mater Sci Rep 5:45
30. Bolse W (1994) Mater Sci Eng R 12:53
31. Jaouen C, Riviere JP, Bellara A, Delafond J (1984) Nucl Inst Meth B7/8:591
32. Johnson WL, Cheng YT, Van-Rossum M, Nicolet M-A (1985) Nucl Inst Meth B7/8:657
33. BØrgesen P, Lilienfeld DA, Johnson HH (1990) Appl Phys Lett 57(14):1407
34. BØrgesen P, Lilienfeld DA, Msaad H (1991) Nucl Inst Meth B59/60:563
35. Saleh NS, Al-Saleh KA, Saleh AA (1990) Nucl Inst Meth B47:263